Original Article

A new dynamic myocardial phantom for the assessment of left ventricular function by gated single-photon emission tomography

Naoki Kubo[1], Koichi Morita[2], Chietsugu Katoh[3], Tohru Shiga[2], Masanori Konno[2], Eriko Tsukamoto[2], Yutaka Morita[1,], Nagara Tamaki[2]

1 Department of Radiological Technology, College of Medical Technology, Hokkaido University, Sapporo, Japan

2 Department of Nuclear Medicine, School of Medicine, Hokkaido University, Sapporo, Japan

3 Department of Tracer Kinetics, Hokkaido University, Sapporo, Japan

Abstract. Gated myocardial perfusion single-photon emission tomography (SPET) has been used for the measurement of left ventricular (LV) function and validated by means of comparison with other imaging modalities. We have designed a new dynamic myocardial phantom in order to validate the LV function as assessed by the use of gated myocardial perfusion SPET. The phantom consists of two half-ellipsoids (an endocardial surface and an epicardial surface) and a thorax. The myocardial space is filled with a radioactive solution. The endocardial surface moves continuously towards and away from the epicardial surface in the longitudinal axis to vary the LV volume [143 ml at end-diastole (ED), 107 ml at end-systole (ES)] and thickness (apex 8 mm at ED and 26 mm at ES, midplane 8 mm). The mean values of wall motion (WM) for the apical midplane region and the basal midplane region were 5 mm and 2 mm, respectively. Gated myocardial SPET was performed during 8 and 16 intervals. These projection data sets were processed using a Butterworth filter with an order of 5 and a critical frequency of 0.34 cycles/cm. LV function was calculated using the quantitative gated SPET (QGS) algorithm. The LV function values estimated by gated SPET during 16 intervals [22% for ejection fraction (EF), 3.7 mm for WM of the apical midplane, 1.7 mm for WM of the basal midplane] closely resembled actual LV functions [25% for EF, 5 mm for WM of the apical midplane, 2 mm for WM of the basal midplane]. However, the estimated values during 8 intervals were smaller than those during 16 intervals (19% for EF, 3.3 mm for WM of the apical-midplane, 1.1 mm for WM of the basal-midplane). The estimated LV volumes closely correlated

with the actual volumes (r = 0.99 for 16 intervals, r = 0.95 for 8 intervals). Utilizing this phantom, LV function estimated using gated myocardial SPET can be compared with actual values.

Key words. Myocardium - Phantom - Wall motion - Single-photon emission tomography

Introduction

The assessment of left ventricular (LV) volumes and LV function is of importance for both diagnosis and prognosis [1, 2, 3, 4, 5]. Gated myocardial perfusion single-photon emission tomography (SPET) has been used to assess LV function and volumes [6, 7, 8, 9, 10, 11, 12, 13, 14] and allows for simultaneous determination of both myocardial perfusion and function in a single study. The accuracy of LV functional measurement has been validated by means of comparison with other imaging modalities [15, 16, 17, 18, 19, 20, 21, 22, 23, 24, 25, 26, 27, 28].

We have developed a new moving myocardial phantom to validate the values calculated by the use of gated SPET. This myocardial phantom consists of a fixed epicardial surface and an endocardial surface which continuously moves towards and away from the epicardial surface to change the LV volume.

In this study we assessed the LV functional parameters estimated from gated SPET with this dynamic myocardial phantom.

Materials and methods

Phantom design. The phantom consists of two half-ellipsoids and a thorax. The half-ellipsoids are modelled as an endocardial surface and an epicardial surface. The ellipsoid representing the epicardial surface has a half major axis of 92 mm and a minor axis of 64 mm. The ellipsoid representing the endocardial surface has a half major axis of 81 mm and a minor axis of 48 mm (Fig. 1). Supply tubes containing radioactive solution were connected to the basal anterior epicardial surface.

The thorax phantom is constructed to represent the lungs, a mediastinum and spine [29]. The sections representing the lungs contain beads of foaming polystyrene and

water, and have a density of 0.28 g/cm3. The mediastinal section contains water (density 1.0 g/cm3). The spinal section is constructed of a material having a density of 1.27 g/cm3 (Fig. 2).

The myocardial phantom is located in the mediastinum. The myocardial longitudinal axis is bent backward at 24° and rightward at 40° with the thorax axial (Figs. 2, 3).

The endocardial surface moves continuously towards and away from the epicardial surface along the longitudinal axis. The stroke length is 18 mm (Figs. 1, 4). Consequently, the LV volume changes from 107 ml (ES) to 143 ml (ED) and the thickness also changes (apex 8 mm at ED and 26 mm at ES). This phantom has a trigger generator which outputs 2-mV pulse in the ED phase.

SPET acquisition. The myocardial space of the phantom was filled with 143 kBq/ml of technetium-99m solution. SPET was acquired on a dual-detector camera (Vertex, ADAC Laboratories) with the detectors oriented at 90°. The camera was equipped with low-energy (VXGP) collimators, with the photopeak centered at 140 keV and a ±10% window. Step-and-shoot detector rotation was employed, with 32 projections over 180° (RAO 45° to LPO 45°, non-circular orbit for the nearest-neighbour distances) and 15 s of data collection per projection, distributed over 16 cardiac frames. In this phantom study, the cardiac cycle was 40 cycles/min. Data were acquired in a 64×64 matrix. The 16 intervals at each projection angle were compacted into 8.

Data processing. The 8- and 16-interval projection data were processed using a Butterworth filter with an order of 5 and a critical frequency of 0.38 cycles/cm. The ramp filter was used for reconstruction with filtered backprojection. Scatter and attenuation corrections were not performed. The transaxial images were reoriented into short-axis images. The 8- and 16-interval LV function was calculated from short-axis

images using the quantitative gated SPET (QGS) algorithm developed by Germano et al. [30, 31, 32, 33]. Estimated LV function was based on LV volumes, ejection fraction (EF%) and wall motion (WM). Estimated WM was calculated by using the mean values of the apical midplane and basal midplane regions from the QGS results.

Actual LV volumes during each phase were calculated based on the stroke length during each phase. Actual WM was based on the perpendicular length between the ED endocardial surface and the ES endocardial surface. The mean values of WM were 5 mm at the apical midplane region and 2 mm at the basal midplane region (Fig. 4).

The apical and basal regions were excluded from this study.

Results

SPET images

The SPET images of the dynamic myocardial phantom are shown in Fig. 5. The phantom cavity was smaller during the ES phase than during the ED phase. Myocardial activity during the ES phase was greater than during the ED phase. No definite regional perfusion defects were seen in the SPET images.

LV volumes and ejection fraction

The estimated LV volumes for both 8 and 16 intervals were highly correlated with the actual volumes ($y = 13 + 0.63x$, $r = 0.99$, SEE = 1.3 ml with 16 intervals, $y = 23 + 0.54x$, $r = 0.95$, SEE = 2.4 ml with 8 intervals).

The time-volume curves for 8 intervals and 16 intervals are shown in Fig. 6.

The actual EF of this phantom was 25%. The estimated EF was 22% for 16 intervals and 19% for 8 intervals (Table 1).

Wall motion

The estimated WM was also compared with the actual WM (Table 1). The measurements obtained in this study revealed differences in WM between the apical midplane and the basal midplane. The estimated WM during 8 intervals was slightly smaller than the estimated WM during 16 intervals in both the apical midplane and the basal midplane.

Discussion

Phantom design and SPET images

The results of this study indicate that LV function can be calculated by gated SPET and validated using our new dynamic myocardial phantom. A feature of this phantom is its ability to reproduce thickening, which is an important mechanism of myocardium. The phantom is able to simulate wall motion of the endocardial surface and LV volumes can be varied. It is also to be noted that the functional parameters of the phantom are known, as a consequence of which it will be valid for every algorithm of LV functional measurements.

This phantom reproduces attenuation and scatter. When the phantom is attached to diaphragmatic and breast models, phantom studies can reveal the effect of attenuation and scatter for LV functional measurements. Furthermore, if a spacer is inserted into a space between the epicardial and endocardial surface, a study resembling a myocardial defect can be performed.

This phantom approximates the actual anatomical location of the myocardium, as well as myocardial size and shape. Accordingly, SPET imaging of the phantom reproduces clinical studies. In addition, SPET included an obstacle causing collimator blurring similar to that found in a clinical study. However, estimated LV functions corresponded

closely with actual functions, and estimated LV volumes correlated with actual volumes. The reason for this is that the QGS algorithm works in three-dimensional space. A spatial blur on the SPET spreads in three-dimensional space. If the short-axis images were to be analysed in two-dimensional space, the influence of the blur on the longitudinal axis could not be considered. If the SPET study of the phantom were not processed using an algorithm capable of working in three dimensions, the estimated LV functions would differ from the actual values.

LV volumes and ejection fraction

All LV volumes were underestimated. The reason for this may have been limited spatial resolution. Germano et al. reported that lower critical frequency effects a degradation of spatial resolution which causes a reduction in estimated LV volume [30].

On the other hand, the regression equation obtained from this study nearly reproduces the LV volume of the original experiment by Germano et al. In their experiment, the cavity volume of the phantom was 63 ml. When the actual volume is 63 ml, the calculated volume will be 57 ml on the 8-interval regression equation. Thus, the aforementioned underestimation may be significantly reduced in the range of 50-60 ml.

The ED volume was underestimated to a greater extent than the ES volume. The reason for this is as follows: Partial volume effect and spillover adversely affect the quantification of radioactivity concentration in small objects [34]. Hoffman et al. reported that image bar thickness overestimation increases with true bar thickness thinning [35]. The myocardial thickness during the ED phase was smaller than that during the ES phase. Accordingly, the error in myocardial thickness at ED was greater than that at ES. Overestimating the myocardial thickening caused a reduction in LV volumes.

The time-volume curves resembled a cosine wave. Since the stroke motion of this phantom is very simple, these curves are different from a clinical time-volume curve in which systolic contractions are rapid and diastolic expansion is slower [36, 37]. However, it was possible to detect differences in measurements between 8 and 16 intervals.

It has been reported that compacting 16-interval data sets into 8-interval data sets is equivalent to smoothing the time-volume curve [30]. This finding was confirmed by the present study using this dynamic phantom. It was demonstrated that LV volumes during 16 intervals were closer to the actual volumes than those during 8 intervals.

The EF of this phantom is lower than a normal EF. However, this phantom's EF can be calculated by gated SPET.

Wall motion

The WM of the apical region was excluded from this study because the WM of the apical region has a length of more than 10 mm, which is higher than the limit for QGS. With QGS, motion greater than 10 mm is assumed to equal 10 mm (the scale is "saturated" at 10 mm). Since the basal region was connected to the radioactive solution supply tubes, WM of the basal region was also excluded from this study.

All estimates of WM for 8 intervals were smaller than those for 16 intervals. Because compacting 16-interval data sets into 8-interval data sets is equivalent to smoothing all images during a phase, the acquired myocardial SPET images during 8 intervals were more blurred than those acquired during 16 intervals, with thicker myocardium at ED. The estimated myocardial wall at ED was thicker. Such a blurring effect may cause underestimation of wall motion during 8 intervals.

Limitations of this study

Using the described dynamic phantom it was not possible to evaluate LV volume over a

wide range. However, gated SPET has been fully tested in comparison with echocardiography, magnetic resonance imaging, contrast ventriculography and other modalities. This study focussed on the extent of differences in estimated LV volume and regional functional parameters with the dynamic myocardial phantom, which provides known parameters.

The relationship between perfusion defects and estimated functional parameters using a digital phantom has been investigated in detail [31]. The location and size of perfusion defects can be easily varied in a digital phantom simulation. On the other hand, experiments with respect to perfusion defects using our dynamic phantom require the production of a spacer for the defect, the insertion of the spacer, SPET acquisition and SPET processing. Nevertheless, experiments using our dynamic phantom yield results similar to those obtained with the digital phantom simulation.

This dynamic phantom differs from the physiological cardiac cycle in that the entire radioactivity within one interval increases during the phantom's systole, whereas myocardial radioactivity in the physiological cardiac cycle remains constant. However, this may be a minor problem. In gated myocardial perfusion SPET, SPET values during the ES phase increase compared with those during the ED phase owing to partial volume effects but not to an actual increase in myocardial radioactivity. The major reason for the volume underestimation in our study was related to an interaction of spatial blur and partial volume effects. To minimise partial volume effects, a new technical study with a perfect acquisition with minimum pixel size, a large number of counts and ultra-high-resolution collimators is warranted.

Conclusion

We have developed a dynamic myocardial phantom in order to validate the values calculated by gated SPET. Utilizing this phantom, some differences in measurements with different acquisition parameters were identified. Thus, use of the dynamic myocardial phantom validates influences associated with the acquisition parameters (the number of intervals), and permits comparison of LV function values estimated using gated myocardial SPET and actual values.

References

1. De Feyter PJ, van Eenige MJ, Dighton DH, Visser FC, de Jong J, Roos JP. Prognostic value of exercise testing, coronary angiography and left ventriculography 6-8 weeks after myocardial infarction. *Circulation* 1982; 66: 527-536.
2. Roubin GS, Harris PJ, Bernstein L, Kelly DT. Coronary anatomy and prognosis after myocardial infarction in patients 60 years of age and younger. *Circulation* 1983; 67: 743-749.
3. Gill JB, Moore RH, Tamaki N, Miller DD, Barlai-Kovach M, Yasuda T, Boucher CA, Strauss HW. Multigated blood-pool tomography: new method for the assessment of left ventricular function. *J Nucl Med* 1986; 27: 1916-1924.
4. White HD, Norris RM, Brown MA, Brandt PW, Whitlock RM, Wild CJ. Left ventricular end-systolic volume as the major determinant of survival after recovery from myocardial infarction. *Circulation* 1987; 76: 44-51.
5. Nichols K, Tamis J, DePuey EG, Mieres J, Malhotra S, Rozanski A. Relationship of gated SPECT ventricular function parameters to angiographic measurements. *J Nucl Cardiol* 1998; 5: 295-303.
6. Smith WH, Kastner RJ, Calnon DA, Segalla D, Beller GA, Watson DD. Quantitative gated single photon emission computed tomography imaging: a counts-based method for display and measurement of regional and global ventricular systolic function. *J Nucl Cardiol* 1997; 4: 451-463.
7. Everaert H, Bossuyt A, Franken PR. Left ventricular ejection fraction and volumes from gated single photon emission tomographic myocardial perfusion images:

comparison between two algorithms working in three-dimensional space. *J Nucl Cardiol* 1997; 4: 472-476.

8. Berman DS, Germano G. Evaluation of ventricular ejection fraction, wall motion, wall thickening, and other parameters with gated myocardial perfusion single-photon emission computed tomography. *J Nucl Cardiol* 1997; 4: S169-S171.
9. Germano G, Erel J, Kiat H, Kavanagh PB, Berman DS. Quantitative LVEF and qualitative regional function from gated thallium-201 perfusion SPECT. *J Nucl Med* 1997; 38: 749-754.
10. Maunoury C, Chen CC, Chua KB, Thompson CJ. Quantification of left ventricular function with thallium-201 and technetium-99m-sestamibi myocardial gated SPECT. *J Nucl Med* 1997; 38:958-961.
11. Everaert H, Vanhove C, Franken PR. Gated SPET myocardial perfusion acquisition within 5 minutes using focussing collimators and a three-head gamma camera. *Eur J Nucl Med* 1998; 25: 587-593.
12. Germano G. Automatic analysis of ventricular function by nuclear imaging. *Curr Opin Cardiol* 1998; 13: 425-429.
13. Paul AK, Hasegawa S, Yoshioka J, Tsujimura E, Yamaguchi H, Tokita N, Maruyama A, Xiuli M, Nishimura T. Exercise-induced stunning continues for at least one hour: evaluation with quantitative gated single-photon emission tomography. *Eur J Nucl Med* 1999; 26: 410-415.
14. Anagnostopoulos C, Underwood SR. Simultaneous assessment of myocardial perfusion and function: how and when? *Eur J Nucl Med* 1998; 25: 555-558.
15. DePuey EG, Nichols K, Dobrinsky C. Left ventricular ejection fraction assessed from gated technetium-99m-sestamibi SPECT. *J Nucl Med* 1993; 34: 1871-1876.

16. Williams KA, Tailon LA. Left ventricular function in patients with coronary artery disease assessed by gated tomographic myocardial perfusion images. Comparison with assessment by contrast ventriculography and first-pass radionuclide angiography. *J Am Coll Cardiol* 1996; 27: 173-181.
17. Everaert H, Franken PR, Flamen P, Goris M, Momen A, Bossuyt A. Left ventricular ejection fraction from gated SPET myocardial perfusion studies: a method based on the radial distribution of count rate density across the myocardial wall. *Eur J Nucl Med* 1996; 23: 1628-1633.
18. Calnon DA, Kastner RJ, Smith WH, Segalla D, Beller GA, Watson DD. Validation of a new counts-based gated single photon emission computed tomography method for quantifying left ventricular systolic function: comparison with equilibrium radionuclide angiography. *J Nucl Cardiol* 1997; 4: 464-471.
19. Mochizuki T, Murase K, Tanaka H, Kondoh T, Hamamoto K, Tauxe WN. Assessment of left ventricular volume using ECG-gated SPECT with technetium-99m-MIBI and technetium-99m-tetrofosmin. *J Nucl Med* 1997; 38: 53-57.
20. Hambye AS, Dobbeleir A, Vervaet A, Chi-Chou H. Can we rely on $^{99}Tc^{m}$-sestamibi gated tomographic myocardial perfusion imaging to quantify left ventricular function? A comparative study with classical isotopic techniques for the measurement of ejection fraction. *Nucl Med Commun* 1997; 18: 751-760.
21. Yang KT, Chen HD. Evaluation of global and regional left ventricular function using technetium-99m sestamibi ECG-gated single-photon emission tomography. *Eur J Nucl Med* 1998; 25: 515-521.

22. Stollfuss JC, Haas F, Matsunari I, Neverve J, Nekolla S, Schneider-Eicke J, Schricke U, Ziegler S, Schwaiger M. Regional myocardial wall thickening and global ejection fraction in patients with low angiographic left ventricular ejection fraction assessed by visual and quantitative resting ECG-gated ^{99m}Tc-tetrofosmin single-photon emission tomography and magnetic resonance imaging. *Eur J Nucl Med* 1998; 25: 522-530.
23. Iskandrian AE, Germano G, VanDecker W, Ogilby JD, Wolf N, Mintz R, Berman DS. Validation of left ventricular volume measurements by gated SPECT ^{99m}Tc-labeled sestamibi imaging. *J Nucl Cardiol* 1998; 5: 574-578.
24. Anagnostopoulos C, Gunning MG, Pennell DJ, Laney R, Proukakis H, Underwood SR. Regional myocardial motion and thickening assessed at rest by ECG-gated ^{99m}Tc-MIBI emission tomography and by magnetic resonance imaging. *Eur J Nucl Med* 1996; 23: 909-916.
25. Yamashita K, Tamaki N, Yonekura Y, Ohtani H, Saji H, Mukai T, Kambara H, Kawai C, Ban T, Konishi J. Quantitative analysis of regional wall motion by gated myocardial positron emission tomography: validation and comparison with left ventriculography. *J Nucl Med* 1989; 30: 1775-1786.
26. Chua T, Kiat H, Germano G, Maurer G, van Train K, Friedman J, Berman D. Gated technetium-99m sestamibi for simultaneous assessment of stress myocardial perfusion, postexercise regional ventricular function and myocardial viability. Correlation with echocardiography and rest thallium-201 scintigraphy. *J Am Coll Cardiol* 1994; 23: 1107-1114.
27. Vaduganathan P, He ZX, Vick GW 3rd, Mahmarian JJ, Verani MS. Evaluation of left ventricular wall motion, volume, and ejection fraction by gated myocardial

tomography with technetium 99m-labeled tetrofosmin: a comparison with cine magnetic resonance imaging. *J Nucl Cardiol* 1999; 6: 3-10.

28. Faber TL, Akers MS, Peshock RM, Corbett JR. Three-dimensional motion and perfusion quantification in gated single-photon emission computed tomograms. *J Nucl Med* 1991; 32: 2311-2317.
29. Tamaki N. Tl-201 single-photon emission computed tomography (SPECT) [letter to the editor: reply]. *J Nucl Med* 1983; 24: 273-275.
30. Germano G, Kiat H, Kavanagh PB, Moriel M, Mazzanti M, Su H-T, Train KFV, Berman DS. Automatic quantification of ejection fraction from gated myocardial perfusion SPECT. *J Nucl Med* 1995; 36: 2138-2147.
31. Achtert AD, King MA, Dahlberg ST, Pretorius PH, LaCroix KJ, Tsui BM. An investigation of the estimation of ejection fraction and cardiac volumes by a quantitative gated SPECT software package in simulated gated SPECT images. *J Nucl Cardiol* 1998; 5: 144-152.
32. Germano G, Kavanagh PB, Kavanagh JT, Wishner SH, Berman DS, Kavanagh GJ. Repeatability of automatic left ventricular cavity volume measurements from myocardial perfusion SPECT. *J Nucl Cardiol* 1998; 5: 477-483.
33. Germano G, Erel J, Lewin H, Kavanagh PB, Berman DS. Automatic quantitation of regional myocardial wall motion and thickening from gated technetium-99m sestamibi myocardial perfusion single-photon emission computed tomography. *J Am Coll Cardiol* 1997; 30: 1360-1367.
34. Zito F, Gilardi MC, Magnani P, Fazio F. Single-photon emission tomographic quantification in spherical object: effects of object size and background. *Eur J Nucl Med* 1996; 23: 263-271.

35. Hoffman EJ, Huang SC, Phelps ME. Quantitation in positron emission computed tomography. 1. Effect of object size. *J Comput Assist Tomogr* 1979; 3: 299-308.

36. Bhargava V, Slutsky R, Costello D. Peak rate of left-ventricular ejection by a gated radionuclide technique: correlation with contrast angiography. *J Nucl Med* 1981; 22: 506-509.

37. Miller TR, Goldman KJ, Sampathkumaran KS, Biello DR, Ludbrook PA, Sobel BE. Analysis of cardiac diastolic function: application in coronary artery disease. *J Nucl Med* 1983; 24: 2-7.

Fig. 1. Design of the myocardium containing the new dynamic myocardial phantom

Fig. 2. *Top:* design and density of the thorax phantom. *Bottom:* the myocardium location in the thorax phantom

Fig. 3. Anterior view of the dynamic myocardial phantom

Fig. 4. The endocardial location during the end-diastolic phase and end-systolic phases. Apical midplane and basal midplane regions were defined as shown

Fig. 5. SPET images of the dynamic myocardial phantom. the left column shows the ED phase. The right column shows the ES phase (top to bottom: apical, mid and basal short axis, horizontal long-axis and vertical long axis)

Fig. 6. Time-volume curves for 16 intervals and the 8 intervals

Table 1. Comparison of actual values and estimated values

Fig. 1.

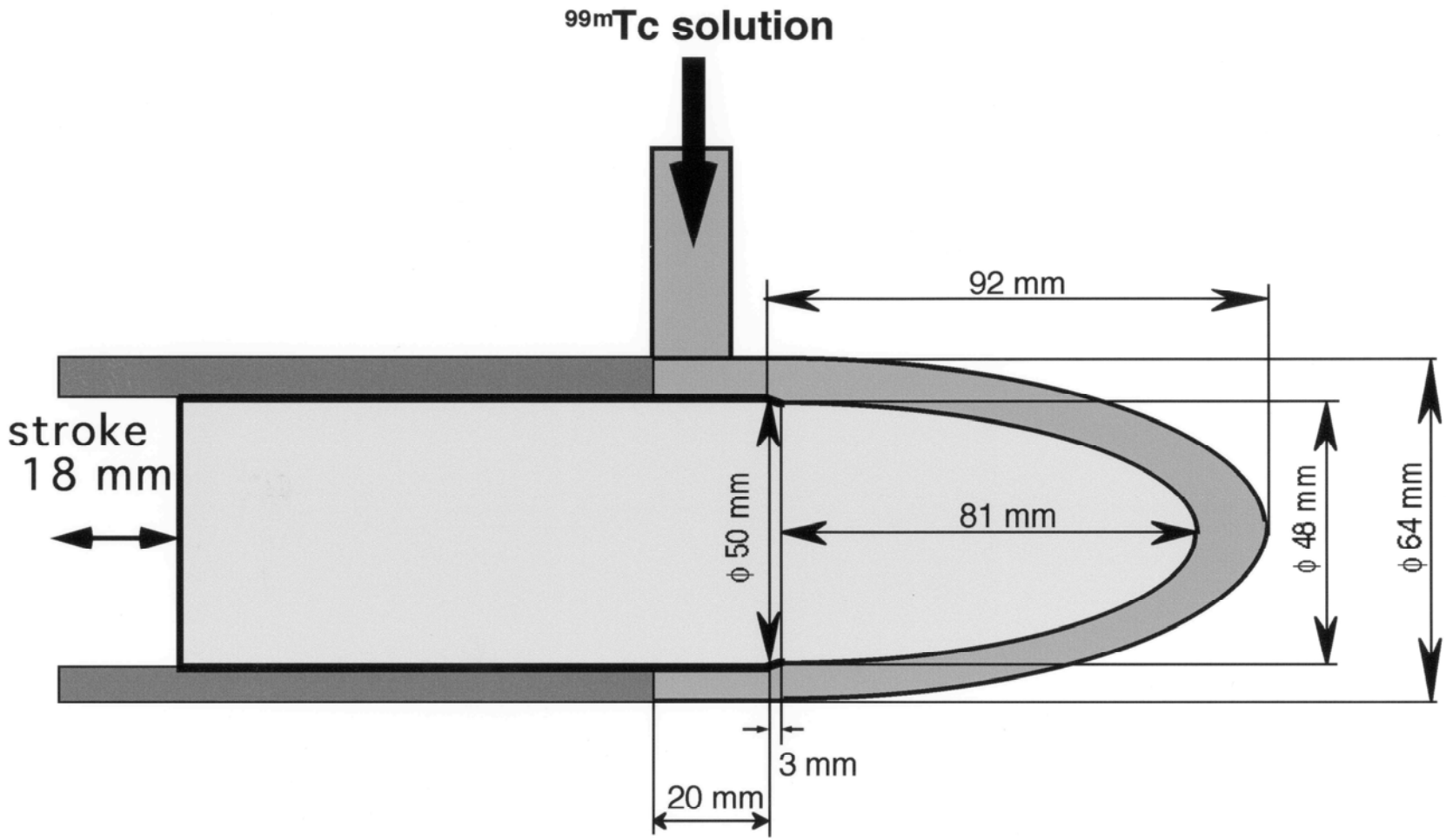
99mTc solution
92 mm
stroke
18 mm
ϕ 50 mm
81 mm
ϕ 48 mm
ϕ 64 mm
3 mm
20 mm

Fig. 2.

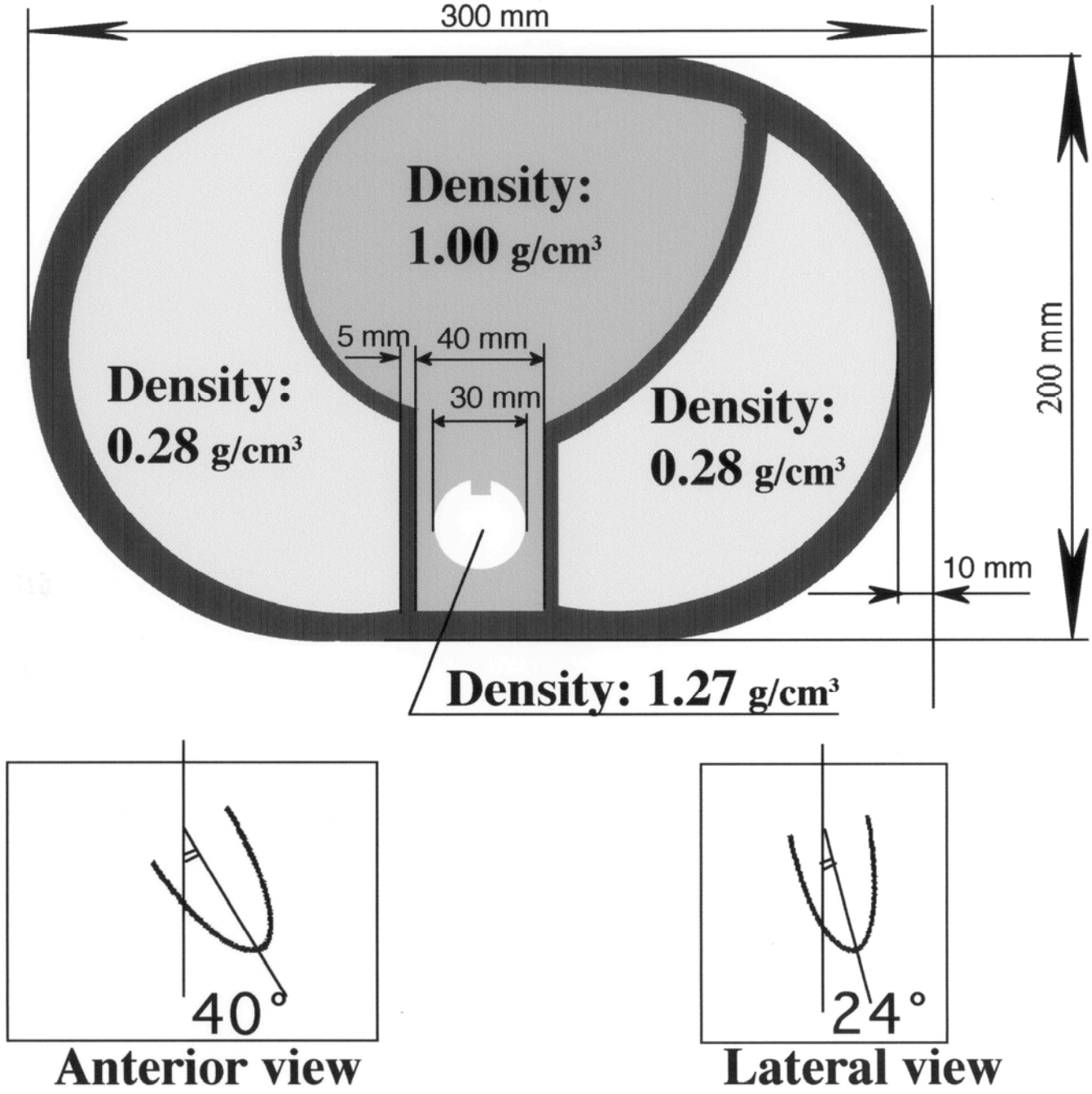
300 mm
Density:
1.00 g/cm³
5 mm
40 mm
30 mm
Density:
0.28 g/cm³
Density:
0.28 g/cm³
200 mm
10 mm
Density: 1.27 g/cm³
40°
Anterior view
24°
Lateral view

Fig. 3.

Fig. 4.

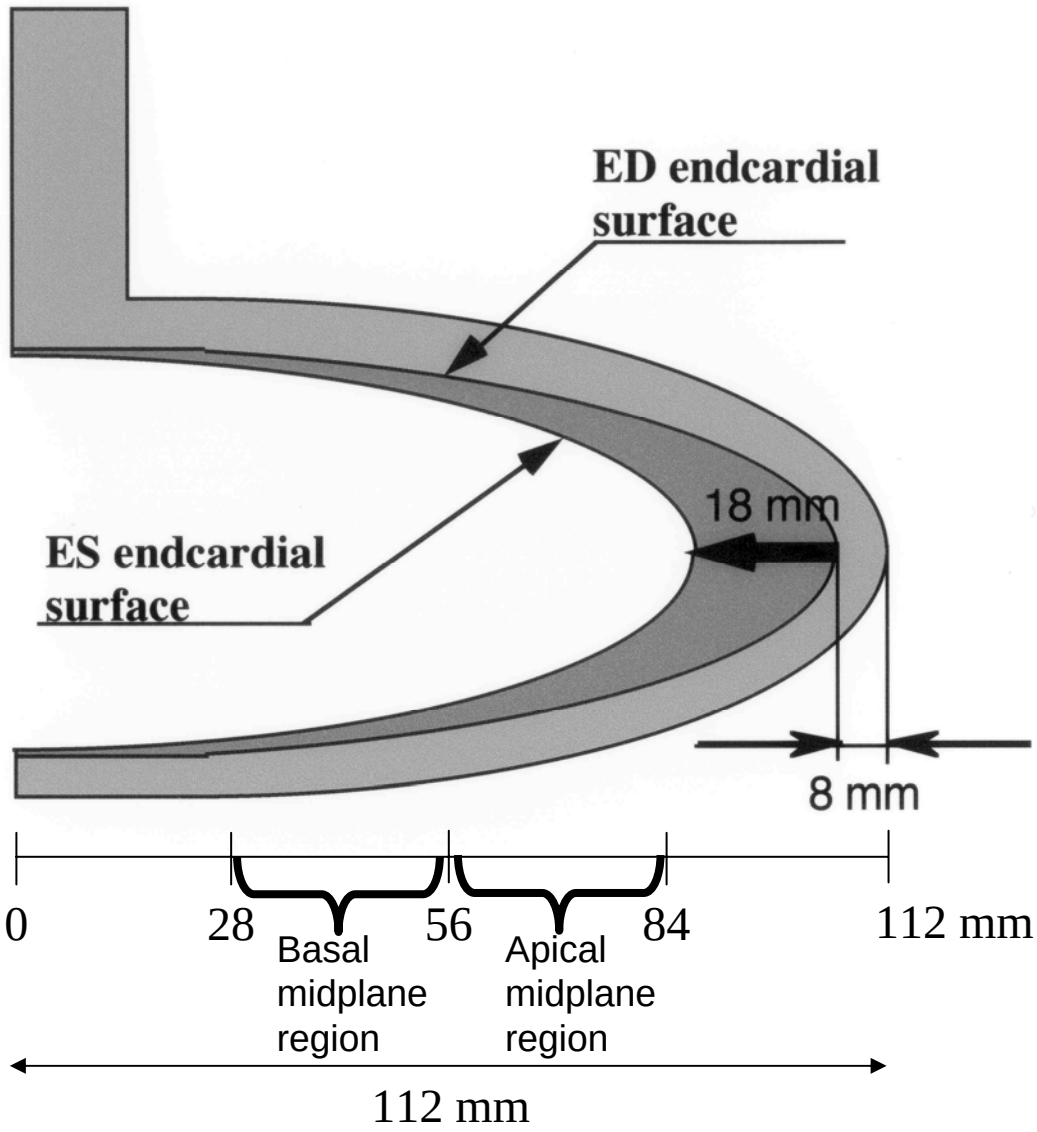
ED endcardial surface
ES endcardial surface
18 mm
8 mm
0
28
56
84
112 mm
Basal midplane region
Apical midplane region
112 mm

Fig. 5.

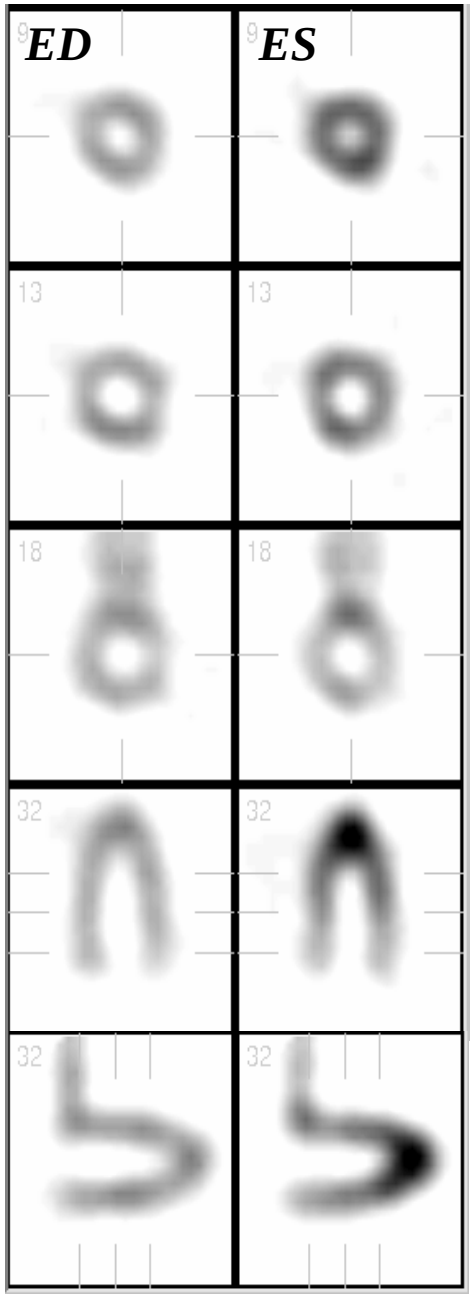

Fig. 6.

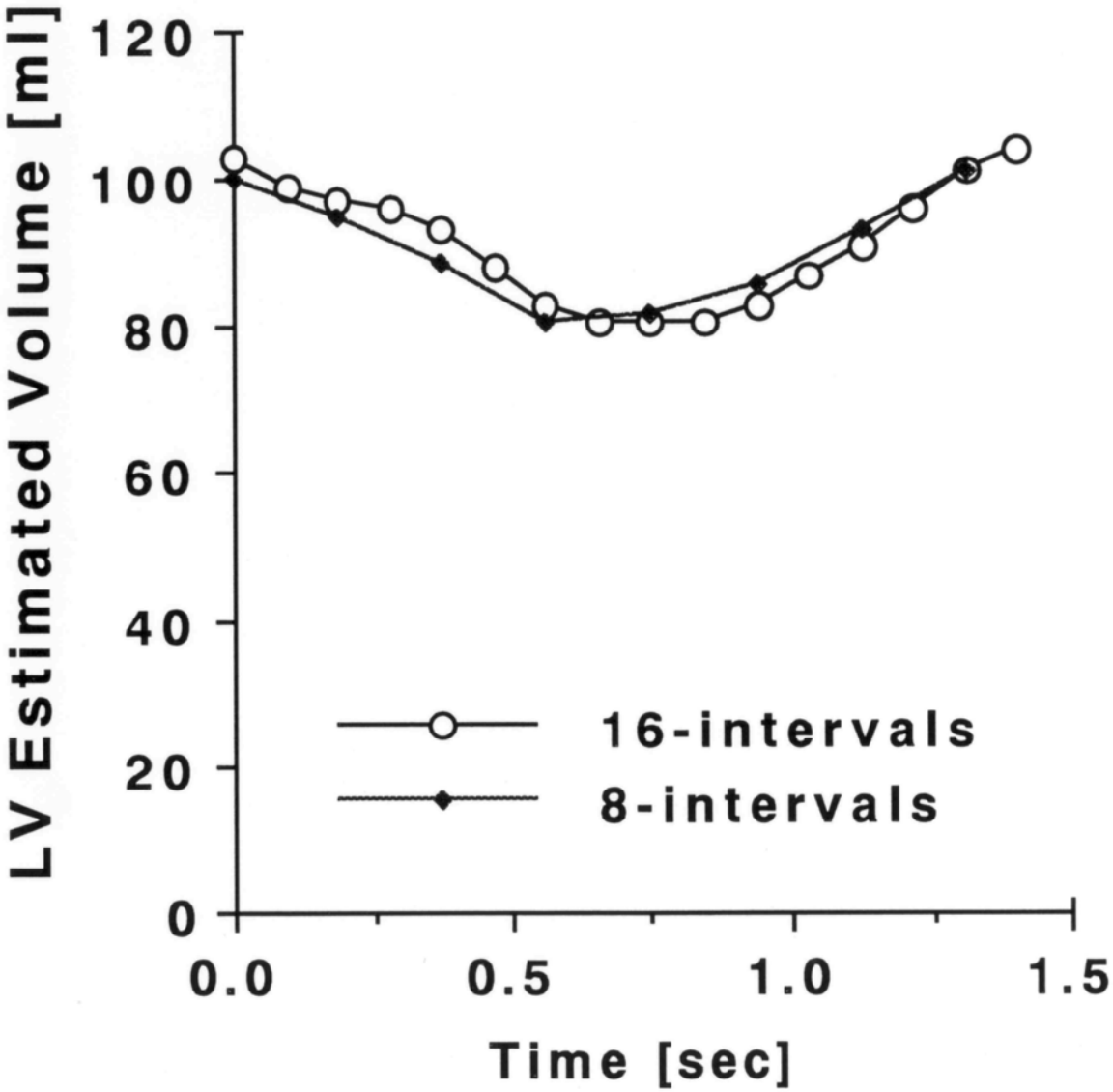
LV Estimated Volume [ml]
120
100
80
60
40
20
0
0.0
0.5
1.0
1.5
Time [sec]
16-intervals
8-intervals

Table 1.

	Actual Value	16 intervals	8 intervals
EDV (ml)	143	104	101
ESV (ml)	107	81	81
SV (ml)	36	23	20
EF (%)	25	22	19
WM ap-m (mm)	5	3.7	3.3
WM ba-m (mm)	2	1.7	1.1

EDV, End-diastolic volume; ESV, end-systolic volume; SV, stroke volume; EF, ejection fraction; WM ap-m, wall motion of the apical midplane; WM ba-m, wall motion of the basal midplane